THE JOURNAL OF PHYSICAL CHEMISTRY B

ARTICLE

pubs.acs.org/JPCB

Scaling between Relaxation, Transport, and Caged Dynamics in Polymers: From Cage Restructuring to Diffusion

F. Puosi[†] and D. Leporini[*,†,‡]

[†]Dipartimento di Fisica "Enrico Fermi", Università di Pisa, Largo B.Pontecorvo 3, I-56127 Pisa, Italy

[‡]IPCF-CNR, UOS Pisa, Italy

ABSTRACT: The slow relaxation, the diffusivity, and the fast cage-dynamics of a melt of fully flexible unentangled polymer chains is studied by molecular-dynamics simulations. States with different nonbonding potential, chain length, density and temperature are considered. The scaling between the slow dynamics and the fast dynamics, as characterized by the amplitude of the rattling motion inside the cage, is evidenced. The analysis carried out in terms of the van Hove function shows that: (i) the scaling does not depend on the specific quantity used to quantify both the relaxation times and the amplitude of the rattling motion; (ii) it holds on the length scale of the jump-like dynamics; (iii) it also holds on the time scale of the diffusive regime if the chain-length effect is taken into proper account, thus extending analogous results already known for atomic liquids.

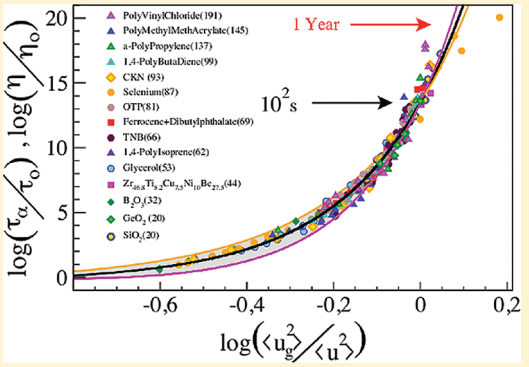

INTRODUCTION

Understanding the extraordinary viscous slow-down that accompanies glass formation is a major scientific challenge.[1−3] On approaching the glass transition (GT), trapping effects are more and more prominent. The average escape time from the cage of the first neighbors, i.e., the structural relaxation time τ_α, increases from a few picoseconds up to thousands of seconds. The rattling motion inside the cage occurs on picosecond time scales with amplitude $\langle u^2\rangle^{1/2}$. This quantity is related to the Debye−Waller factor which, assuming harmonicity of thermal motion, takes the form $\exp(-q^2\langle u^2\rangle/3)$ where q is the absolute value of the scattering vector. Despite the huge range of time scales, older[4] and recent theoretical[2,5−9] studies have addressed the underlying rattling process to understand the structural relaxation gaining support from numerical[10−19] and experimental works on glass-forming liquids[20] and glasses[7,21−26] (for a review, see ref 27).

In a recent paper we reported extensive molecular-dynamics (MD) simulations evidencing the universal scaling between the structural relaxation time and $\langle u^2\rangle$.[28] The findings show that trapping in space (small $\langle u^2\rangle$), resulting in localized fast dynamics, correlates with the slow dynamics (long τ_α). The master curve revealed by the MD scaling procedure is described by a simple parabolic law with respect to $1/\langle u^2\rangle$:[28,30]

$$\tau_\alpha = \tau_0 \exp\left(\frac{\overline{a^2}}{2\langle u^2\rangle} + \frac{\sigma_{a^2}^2}{8\langle u^2\rangle^2}\right) \quad (1)$$

where $\overline{a^2}$ and $\sigma_{a^2}{}^2$ are the average and the variance of the truncated Gaussian distribution of the square displacements to overcome the energy barriers, respectively. Equation 1, when rewritten in terms of reduced $\langle u^2\rangle$, was initially seen to fit with the existing experimental data from supercooled liquids, polymers, and metallic glasses over about eighteen decades of relaxation times and a very wide range of fragilities (Figure 1). Later, the scaling was evidenced in experiments on ionic liquids,[29] as well as simulations of atomic liquids[30] and colloidal gels, the latter being very diluted systems.[31] More recently, the influence of free volume and the proper time scales to observe the genuine fast dynamics have been considered.[29,32] Future work will investigate the pressure dependence of the scaling[33] and the possibility to observe it via suitable probe molecules[34,35] evidencing hierarchical cage dynamics.[36]

The purpose of the present paper is twofold. First, it will be shown that the scaling is robust, i.e., it does not depend severely on the quantity adopted to quantify both the amplitude of the rattling motion of the monomer into the cage of the first neighbors and the relaxation time of the structural relaxation. Moreover, evidence will be provided that the scaling may be extended to include the diffusion regime of the polymer chain. This finding integrates the same result obtained for the atomic liquids.[30]

NUMERICAL METHODS

A coarse-grained model of a melt of linear, fully flexible, unentangled polymer chains with M monomers each is used. The system has $N = 2000$ monomers in all cases, but $M = 3$, where $N = 2001$. Nonbonded monomers at a distance r belonging to the same or different chains interact via the truncated parametric potential:

$$U_{q,p}(r) = \frac{\varepsilon}{q-p}\left[p\left(\frac{\sigma^*}{r}\right)^q - q\left(\frac{\sigma^*}{r}\right)^p\right] + U_{\mathrm{cut}} \quad (2)$$

Special Issue: H. Eugene Stanley Festschrift

Received: April 19, 2011
Revised: July 4, 2011
Published: July 28, 2011

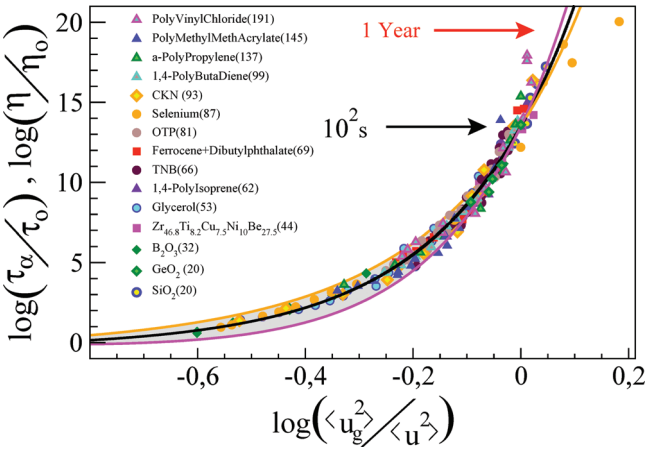

Figure 1. Reduced relaxation time and viscosity versus reduced cage-rattling amplitude ($\langle u_g^2\rangle = \langle u^2(T_g)\rangle$). The numbers in parentheses denote the fragility m. The black curve is eq 1 recast in terms of the reduced cage-rattling amplitude and with parameters $(a^2,\sigma_{a^2}{}^2)$ set by MD simulations.[28,30] The colored curves bound the accuracy of the scaling. Adapted from ref 32 where details about the experiments are given.

where $\sigma^* = 2^{1/6}\sigma$ and the value of the constant U_{cut} is chosen to ensure $U_{q,p}(r) = 0$ at $r \geq r_c = 2.5\sigma$. Changing the p and q parameters does not affect the position $r = \sigma^*$ or the depth ε of the potential minimum, but only the steepness of the repulsive and attractive wings. Bonded monomers interact with a potential that is the sum of the finitely extendible nonlinear elastic (FENE) potential and the Lennard-Jones (LJ) potential.[37] The resulting bond length is $b = 0.97\sigma$ within a few percent. All quantities are in reduced units: length in units of σ, temperature in units of ε/k_B, and time in units of $\sigma(\mu/\varepsilon)^{1/2}$, where μ is the monomer mass. We set $\mu = k_B = 1$. States with different values of the temperature T, the density ρ, the chain length M, and the monomer−monomer interaction potential $U_{q,p}(r)$ are studied; each state is labeled by the multiplet $\{M,\rho,T,p,q\}$. For details on all the investigated states, see ref 30. NPT and NTV ensembles have been used for equilibration runs, while the NVE ensemble has been used for production runs for a given state point. NPT and NTV ensembles are studied by the extended system method introduced by Andersen[38] and Nosé .[39] The numerical integration of the augmented Hamiltonian is performed through the multiple time steps algorithm reversible Reference System Propagator Algorithm (r-RESPA), developed by Tuckerman et al.[40] In particular, the NPT and NTV operators are factorized using the Trotter theorem[41] separating the short-range and long-range contributions of the potential, according to the Weeks−Chandler−Andersen (WCA) decomposition.[42]

QUANTITIES OF INTEREST

One central quantity of the analysis is the self-part of the van Hove function $G_s(\mathbf{r},t)$:[43]

$$G_s(\mathbf{r},t) = \frac{1}{N}\left\langle \sum_{i=1}^{N} \delta[\mathbf{r} + \mathbf{r}_i(0) - \mathbf{r}_i(t)]\right\rangle \quad (3)$$

where $\mathbf{r}_i(t)$ is the position of the ith monomer at time t. In isotropic liquids, the van Hove function depends on the modulus r of $\mathbf{r}$. The interpretation of $G_s(r,t)$ is direct. The product $G_s(r,t)\cdot 4\pi r^2$ is the probability that the monomer is at a distance between r and $r + dr$ from the initial position after a time t. The moments of $G_s(r,t)$ are of interest:

$$\langle r^n(t)\rangle = 4\pi\int_0^\infty r^n G_s(r,t) r^2\, dr \quad (4)$$

or alternatively

$$\langle r^n(t)\rangle = \frac{1}{N}\sum_i \langle ||\mathbf{r}_i(t) - \mathbf{r}_i(0)||^n\rangle \quad (5)$$

For $n = 2$, one recovers the usual mean square displacement (MSD). If the monomer displacement is a Gaussian random variable, $G_s(r,t)$ reduces to the Gaussian form:[43]

$$G_s(r,t) = \left(\frac{3}{2\pi\langle r^2(t)\rangle}\right)^{3/2} \exp\left(-\frac{3r^2}{2\langle r^2(t)\rangle}\right) \quad (6)$$

Equation 6 is the correct limit of $G_s(r,t)$ at very short (ballistic regime, $\langle r^2(t)\rangle = 3k_BT/\mu t^2$) and very long times (diffusion regime, $\langle r^2(t)\rangle = 6Dt$, where D is the monomer diffusion coefficient).

The spatial Fourier transform of the self-part of the van Hove function yields the self-part of the intermediate scattering function (ISF):[43]

$$F_s(q,t) = \int G_s(r,t)\exp(-iq\cdot r)\, dr \quad (7)$$

which, in an isotropic liquid, depends only on the modulus of the wavevector $q = ||\boldsymbol{q}||$ and may be expressed as

$$F_s(q,t) = \frac{1}{N}\left\langle \sum_j^N e^{i\mathbf{q}\cdot(\mathbf{r}_j(t) - \mathbf{r}_j(0))}\right\rangle \quad (8)$$

ISF provides a convenient function to study the rearrangements of the spatial structure of the fluid over the length scale $\sim 2\pi/q$.

RESULTS AND DISCUSSION

General Aspects and Robustness of the Scaling. Figure 2 shows typical MSD and ISF curves of the polymer monomers. ISF is evaluated at $q = q_{max}$, the maximum of the static structure factor ($7.13 \leq q_{max} \leq 7.55$). At very short times (ballistic regime), the MSD increases according to $\langle r^2(t)\rangle \cong (3k_BT/m)t^2$, and the ISF starts to decay. The repeated collisions with the other monomers slow the displacement of the tagged one, as evidenced by the knee of the MSD at $t \sim (12)^{1/2}/\Omega_0 \sim 0.17$, where Ω_0 is an effective collision frequency, i.e., it is the mean small-oscillation frequency of the monomer in the potential well produced by the surrounding ones kept at their equilibrium positions.[44] At later times, a quasi-plateau region, also found in ISF, occurs when the temperature is lowered and/or the density increased. This signals the increased caging of the particle. The latter is released after an average time τ_α, defined by the relation $F_s(q_{max},\tau_\alpha) = e^{-1}$ (for future purposes, one also defines the quantity $\tau_\alpha^{(0.1)}$ via the relation $F_s(q_{max},\tau_\alpha^{(0.1)}) = 0.1$). For $t \gtrsim \tau_\alpha$, MSD increases more steeply. The monomers of short chains ($M \lesssim 3$) undergo diffusive motion, $\langle r^2(t)\rangle = 6Dt$, with D being the chain diffusion coefficient. For longer chains, owing to the increased connectivity, the onset of the diffusion is preceded by a subdiffusive region ($\langle r^2(t)\rangle \propto t^\delta$ with $\delta < 1$, the Rouse regime).[45,46]

The monomer dynamics depends in a complex way on the state parameters. Nonetheless, it is possible to find *distinct* states (labeled by multiplets $\{M,\rho,T,p,q\}$) with *coinciding* MSD and ISF curves from times fairly longer than τ_α down to the crossover to the ballistic regime (picosecond time scale) and even at shorter times if the states have equal temperatures. These states (examples are shown in Figure 2) are obviously characterized

dx.doi.org/10.1021/jp203659r |J. Phys. Chem. B 2011, 115, 14046–14051

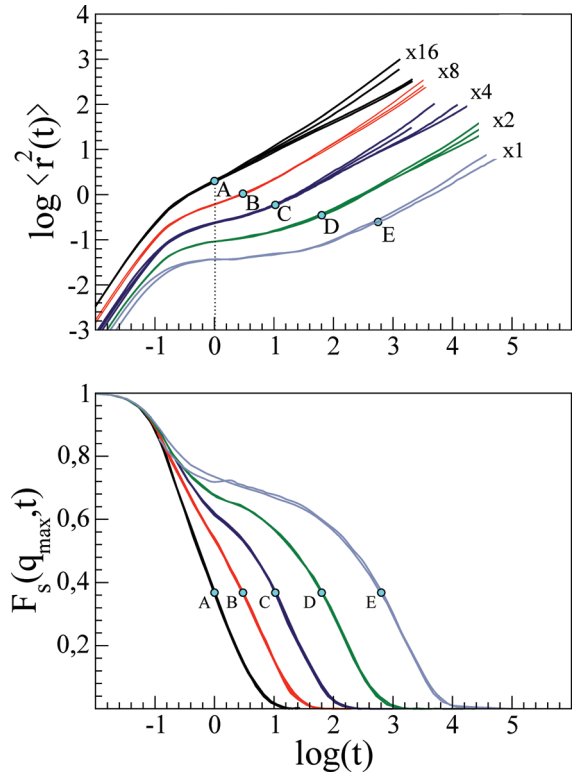

Figure 2. Top: monomer MSD in selected states (M,ρ,T,p,q): set A [(2,1.086,0.7,7,6), (3,1.086,0.7,7,6), (10,1.086,0.7,7,6), (2,1.033,0.7,8,6)]; set B [(2,1.033,0.7,10,6), (3,1.039,0.7,11,6), (3,1.041,0.7,11,6)]; set C [(2,1.033,0.5,10,6), (3,1.056,0.7,12,6), (5,1.033,0.6,12,6), (10,1.056,0.7,12,6)]; set D [(3,1.086,0.7,12,6), (5,1.086,0.7,12,6), (10,1.086,0.7,12,6)]; set E [(2,1.0,0.7,12,11), (3,1.1,1.1,15,7)]. The MSDs are multiplied by indicated factors. Bottom: corresponding ISF. The sets of clustered curves A−E show that, if states have equal τ_α (marked with dots on each curve), the MSD and ISF curves coincide from times fairly longer than τ_α down to the crossover to the ballistic regime at least. Adapted from ref 30.

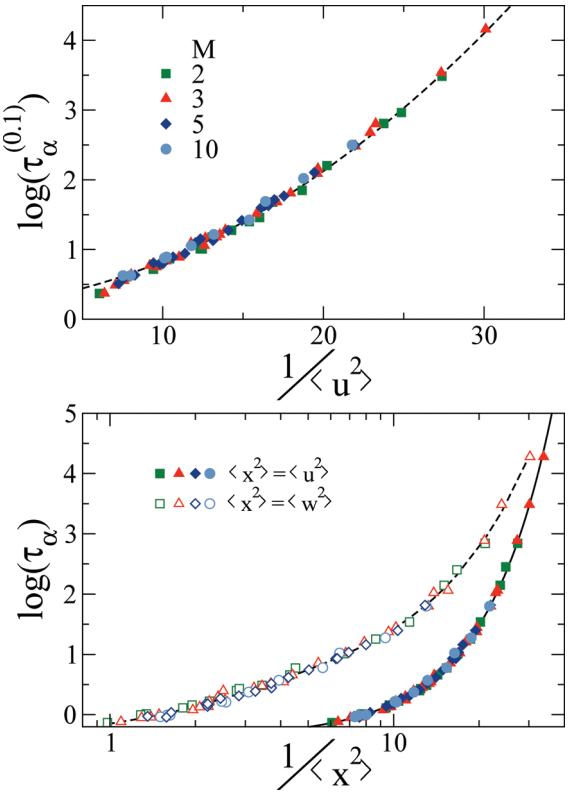

Figure 3. Top: the relaxation time $\tau_\alpha^{(0.1)}$, defined by $F_s(q_{max},\tau_\alpha^{(0.1)}) = 0.1$, versus the ST-MSD $\langle u^2\rangle$. The dashed line is eq 10 with the vertical shift $\alpha' - \alpha = 0.646(2)$. Bottom: the structural relaxation time τ_α versus the ST-MSD evaluated at two different times, $\langle u^2\rangle = \langle r^2(t^*)\rangle$ (filled symbols) and $\langle w^2\rangle = \langle r^2(10\cdot t^*)\rangle$ (open symbols). The solid line across the full symbols is eq 10. The dashed line across the open symbols is a guide for the eyes.

by the same structural relaxation time τ_α. This finding evidences a clear correlation between the caged dynamics and the relaxation behavior. Figure 2 shows that MSD of states with equal τ_α does not collapse for times $t \gg \tau_\alpha$. This is due to the onset of the polymer connectivity effects and the subsequent dependence of the monomer dynamics on the chain length M.[45]

In order to characterize the cage fast dynamics of a given state, we consider MSD evaluated at a characteristic time scale t^* of the rattling motion into the cage defined by the condition that the derivative $\partial \log \langle r^2(t)\rangle/\partial \log t|_{t=t^*}$ is minimum.[28,30] For the present polymer model, $t^* \simeq 1$ in MD units with no appreciable dependence on τ_α.[28,30] Instead, for binary atomic mixtures, t^* increases from about ∼0.7 up to ∼1.9 when τ_α increases from ∼1 to ∼2000.[30] One defines the short-time MSD (ST-MSD) as

$$\langle u^2\rangle \equiv \langle r^2(t = t^*)\rangle \tag{9}$$

This quantity is related to the Debye−Waller factor which, assuming harmonicity of thermal motion, takes the form $\exp(-q^2\langle u^2\rangle/3)$, where q is the absolute value of the scattering vector. For the present polymer model, the structural relaxation time and the ST-MSD collapse on the master curve:[28,30]

$$\log \tau_\alpha = \alpha + \beta\langle u^2\rangle^{-1} + \gamma\langle u^2\rangle^{-2} \tag{10}$$

The best-fit of eq 10, a variant of eq 1, to all the investigated states of the present model yields[28,30] $\alpha = \log \tau_0 = -0.424(1)$, $\beta = a^2/2 \ln 10 = 2.7(1) \times 10^{-2}$, $\gamma = \sigma_{a^2}{}^2/8 \ln 10 = 3.41(3) \times 10^{-3}$.

The scaling between the cage dynamics and the structural relaxation is robust, i.e., it is largely independent of the quantities characterizing the fast MSD dynamics and the structural relaxation. As an example, in Figure 3 the scaling is evidenced by using the two pairs $(\tau^{(0.1)}, \langle u^2\rangle)$ (top panel) or $(\tau_\alpha, \langle r^2(t = 10\cdot t^*)\rangle)$ (bottom panel). For comparison, the original scaling $\log \tau_\alpha$ versus $\langle u^2\rangle^{-1}$ is also shown in Figure 3 (filled symbols). Two remarks about the robustness of the scaling are in order:

(i) The polymer model fulfills the time−temperature superposition principle at long times.[28,30] This readily explains why $\tau^{(0.1)}$ and τ_α are fully equivalent.

(ii) Even if the present model shows that ST-MSD evaluated at both t^* and $10\cdot t^*$ does result in the effective collapse of the data (Figure 3 bottom), in actual experimental cases, the evaluation of ST-MSD at too long times may be dangerous in that spurious relaxation effects may come into play.[29,32]

van Hove Analysis: Length Scales and Jump Dynamics. One issue to be discussed is which length scales are involved in the scaling. Figure 4 compares the self-part of the van Hove function $G_s(r,t)$ evaluated at either the short time t characteristic of the cage rattling (top panel) or τ_α (lower panel) . It is seen that states with equal τ_α (the sets of states labeled as A−E) have

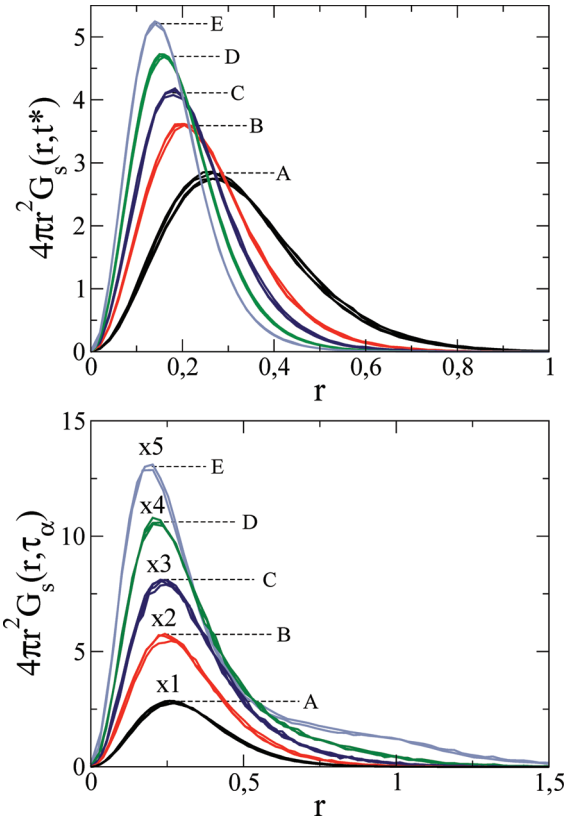

Figure 4. Self-part of the van Hove function $G_s(r,t)$ of the states of Figure 2 at the rattling time $t = t^*$ (top) and the structural relaxation time $t = \tau_\alpha$ (bottom).

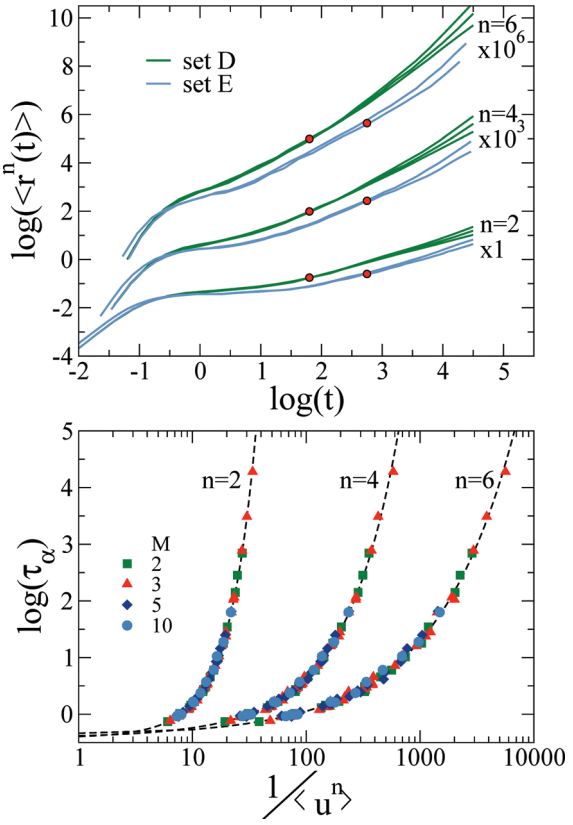

Figure 5. Top: time dependence of the moments of the monomer displacement $\langle r^n(t)\rangle$ with n = 2,4,6 for sets D and E of Figure 2 (the position of τ_α is marked with dots on each curve). Bottom: structural relaxation time τ_α versus $\langle u^n\rangle \equiv \langle r^n(t^*)\rangle$, n = 2,4,6. The dashed lines across the curves are the laws $\log \tau_\alpha = \alpha^{(n)} + \beta^{(n)}\langle u^n\rangle^{-2/n} + \gamma^{(n)}\langle u^n\rangle^{-4/n}$ with $\alpha^{(2)} = \alpha, \beta^{(2)} = \beta$, and $\gamma^{(2)} = \gamma$ as in eq 10, $\alpha^{(4)} = -0.427(2)$, $\beta^{(4)} = 3.7(1) \times 10^{-2}$, $\gamma^{(4)} = 6.93(4) \times 10^{-3}$, $\alpha^{(6)} = -0.425(1)$, $\beta^{(6)} = 4.3(1) \times 10^{-2}$, $\gamma^{(6)} = 1.29(3) \times 10^{-3}$.

coinciding $G_s(r,t^*)$ and $G_s(r,\tau_\alpha)$ within about 3 times the monomer radius. The same coincidence is found for any time in the window $t^* \le t \le \tau_\alpha$ (not shown). Note the shoulders at $r \sim 1$ (the monomer diameter) for states D and E in Figure 4 (bottom). They signal the marked contribution by jump dynamics[47] and show that the latter fulfills the cage scaling too.

This aspect may be further clarified by considering the higher-order moments of the monomer displacement $\langle r^n(t)\rangle$, $n > 2$, which are more sensitive to the large-scale motion than the usual MSD ($n = 2$). In fact, according to eq 4, the coincidence of $G_s(r,t)$ in the window $t^* \le t \le \tau_\alpha$ for states with equal τ_α implies the coincidence of the moments $\langle r^n(t)\rangle$ in the same interval. Figure 5 (top) shows that this is the case for two sets of states and n = 2,4,6 (note that, on increasing n, the chain connectivity becomes increasingly apparent for $t \gtrsim \tau_\alpha$). As a consequence, alternative master curves between the structural relaxation and the higher-order moments of the monomer displacement may be built up (Figure 5, bottom). Note that the coincidence of the moments $\langle r^2(t)\rangle$ and $\langle r^4(t)\rangle$ for $t \le t \le \tau_\alpha$ for states with equal τ_α is expected in view of the coincidence of the nongaussian parameter $\alpha_2(t) = (3\langle r^4(t)\rangle/5\langle r^2(t)\rangle^2) - 1$ in the same time window.[30]

Scaling in the Diffusion Regime of the Chain. The scaling of the diffusive motion with the cage rattling amplitude $\langle u^2\rangle$ has been proven for atomic liquids.[30] For polymers, the situation is more complicated in that, while the structural relaxation is weakly dependent on the chain length,[46] the dynamics for times longer than τ_α does depend.[48] To show this, one defines the relaxation time $\tau_q^{(0.1)}$ via the relation $F_s(q,\tau_q^{(0.1)}) = 0.1$.[49] Figure 6 plots the wave-vector dependence of $\tau_q^{(0.1)}$. It is seen that, when $q \sim 2\pi/\sigma$,

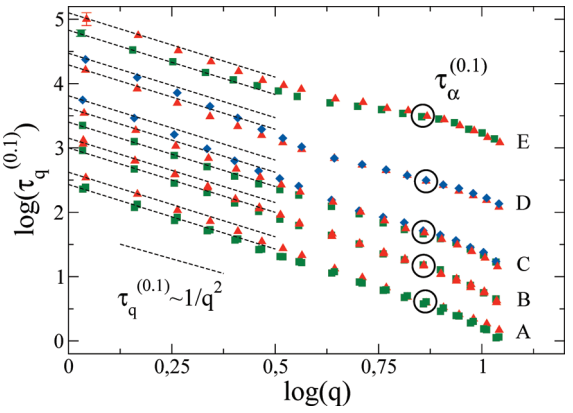

Figure 6. Wave-vector dependence of the relaxation time $\tau_q^{(0.1)}$ for the states of Figure 2 with chain length M = 2,3,5 (same symbols as in Figure 5). Empty circles mark the structural relaxation time $\tau_\alpha^{(0.1)} = \tau_{q_{max}^{(0.1)}}$. For small q values, the diffusive regime is observed, $\tau_q^{(0.1)} \sim q^{-2}$.

the cage length scale is probed, and the relaxation time $\tau_q^{(0.1)} \sim \tau_\alpha^{(0.1)}$ is not dependent on the chain length. When $q \lesssim 2\pi/R_{ee}$, where $R_{ee}^2 = 1.42\ b^2(M-1)$ is the mean square end-to-end distance of the chain,[46] the diffusive regime is observed with $\tau_q^{(0.1)} \propto 1/(Dq^2)$.[48] In this regime, Figure 6 shows that the relaxation

dx.doi.org/10.1021/jp203659r |J. Phys. Chem. B 2011, 115, 14046–14051

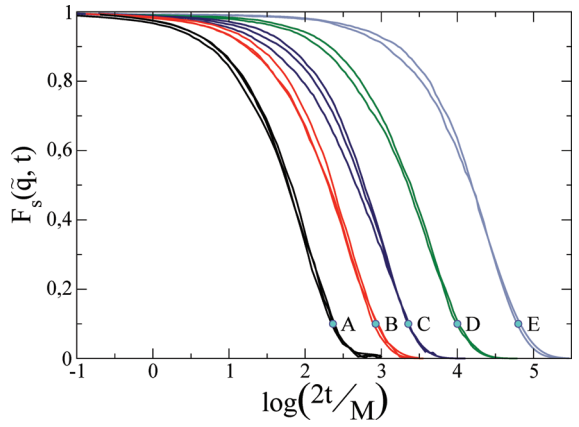

Figure 7. Long-time scaling of $F_s(\tilde{q},t)$ for the states of Figure 2 with M = 2,3,5. $\tilde{q} \approx 1$ is the smallest q vector of our simulations. Circles mark the time $2\tau_D/M$.

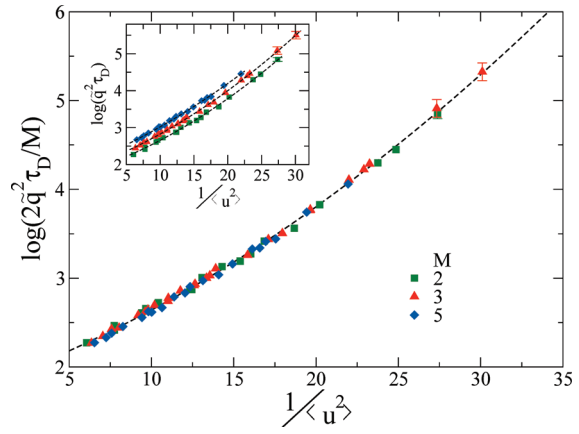

Figure 8. Scaling plot of the reduced diffusion relaxation time τ_D versus ST-MSD $\langle u^2\rangle$ for polymers with different length M. The inset shows the raw data. All the dashed lines are parabolic guides for the eyes.

data are not collapsed on a master curve, even if they are at $q \sim 2\pi/\sigma \sim q_{max}$, i.e., the original form of the scaling of the structural relaxation time, which does not take into account the chain length M in any respect, does not work. It must be noted that the onset of the diffusive behavior for small q values occurs not far from q_{max} because the chains are very short. For longer chain length M, this behavior is observed at smaller q values with $q \lesssim 2\pi/R_{ee} \simeq 2\pi/(b(M-1)^{1/2})$. Furthermore, in the Rouse region where the chain entanglements are negligible, i.e., $M \lesssim 32$,[37] a new scaling law, $\tau_q^{(0.1)} \sim q^{-4}$, becomes apparent for $2\pi/R_{ee} \lesssim q \lesssim q_{max}$ due to the relaxation of the chain conformation.[37]

To extend the scaling to the diffusive regime of polymers, one defines the diffusion relaxation time:

$$\tau_D \equiv \lim_{q \to 0} \tau_q^{(0.1)} \qquad (11)$$

In practice, it is enough to consider $q \lesssim 2\pi/(R_{ee})^{1/2}$. Figure 7 plots ISF at $\tilde{q}$, the smallest q vector of our simulations, and considers the set of states A−E with equal structural relaxation time and chain length M = 2,3,5 (see Figure 2). It is seen that the decay at long times collapses by using the reduced time t/M. This is readily explained since $\tau_D \propto 1/(D\,q^2)$ and for short unentangled chains $D \propto M^{-1}$.[37,48] However, it must be noted that

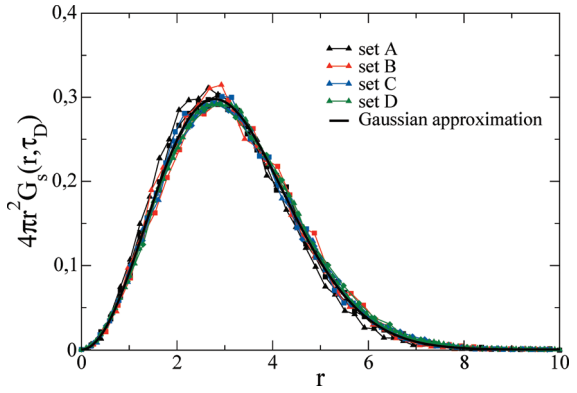

Figure 9. van Hove function $G_s(r,t)$ for $t = \tau_D$ of the states in Figure 2 with chain length M = 2,3,5. The master curve is the Gaussian approximation, eq 6.

deviations from the previous scaling law are seen at lower temperatures than the ones of the present study.[50]

We are now in a position to show that the polymer diffusion regime exhibits scaling with the ST-MSD $\langle u^2\rangle$. Figure 8 plots the reduced quantity $2\tilde{q}^2\tau_D/M$, proportional to ζ/T, with ζ being the monomer friction coefficient,[48] versus the ST-MSD $\langle u^2\rangle$. It is seen that, when the effects due to the chain length are properly treated, the scaling holds even at the very long times of polymer diffusion. This finding complements the analogous result obtained for the diffusion of atomic mixtures.[30]

To complete the characterization of the diffusive regime, Figure 9 shows the van Hove function evaluated at τ_D for the states belonging to sets A−D with chain length M = 2,3,5 (see Figure 2). As expected, all the curve collapse on the same master curve, which is well approximated by the Gaussian approximation (eq 6).

CONCLUSIONS

The results of extensive MD simulations of a melt of fully flexible unentangled polymer chains have been presented. States with different nonbonding potential, chain length, density, and temperature are considered. Strong correlations between the slow relaxation, the diffusivity, and the fast cage dynamics are evidenced and scaled on well-defined master curves. The novel results on the scaling are:

(i) It does not depend on the specific quantity used to quantify both the relaxation times and the amplitude of the rattling motion.
(ii) It works on the length scale of the jump-like dynamics.
(iii) It reaches the time scales of the diffusive regime of the polymer chain, thus extending to connected systems analogous results known for atomic liquids.

AUTHOR INFORMATION

Corresponding Author
*E-mail: dino.leporini@df.unipi.it.

ACKNOWLEDGMENT

Computational resources by "Laboratorio per il Calcolo Scientifico", Department of Physics "Enrico Fermi", Pisa, are gratefully acknowledged.

REFERENCES

(1) Angell, C. *J. Non-Cryst. Solids* **1991**, *131*−*133*, 13–31.
(2) Angell, C. A. *Science* **1995**, *267*, 1924–1935.
(3) Debenedetti, P. G.; Stillinger, F. H. *Nature* **2001**, *410*, 259–267.
(4) Tobolsky, A.; Powell, R. E.; Eyring, H. Elastic-viscous properties of matter. In*Frontiers in Chemistry*; Burk, R. E., Grummit, O., Eds.; Interscience: New York, 1943; pp 125−190.
(5) Hall, R. W.; Wolynes, P. G. *J. Chem. Phys.* **1987**, *86*, 2943–2948.
(6) Dyre, J. C.; Olsen, N. B.; Christensen, T. *Phys. Rev. B* **1996**, *53*, 2171–2174.
(7) Martinez, L.-M.; Angell, C. A. *Nature* **2001**, *410*, 663–667.
(8) Ngai, K. L. *Philos. Mag.* **2004**, *84*, 1341–1353.
(9) Ngai, K. L. *J. Non-Cryst. Solids* **2000**, *275*, 7–51.
(10) Angell, C. A. *J. Am. Chem. Soc.* **1968**, *86*, 117–124.
(11) Nemilov, S. V. *Russ. J. Phys. Chem.* **1968**, *42*, 726–729.
(12) Shao, J.; Angell, C. A. Vibrational anharmonicity and the glass transition in strong and fragile vitreous polymorphs. *Proc. XVIIth Int. Congr. Glass, Beijing* **1995**, 311–320.
(13) Starr, F.; Sastry, S.; Douglas, J. F.; Glotzer, S. *Phys. Rev. Lett.* **2002**, *89*, 125501.
(14) Bordat, P.; Affouard, F.; Descamps, M.; Ngai, K. L. *Phys. Rev. Lett.* **2004**, *93*, 105502.
(15) Widmer-Cooper, A.; Harrowell, P. *Phys. Rev. Lett.* **2006**, *96* (4), 185701.
(16) Zhang, H.; Srolovitz, D. J.; Douglas, J. F.; Warren, J. A. *Proc. Natl. Acad. Sci. U.S.A.* **2009**, *106*, 7735–7740.
(17) Widmer-Cooper, A.; Perry, H.; Harrowell, P.; Reichman, D. R. *Nat. Phys.* **2008**, *4*, 711–715.
(18) Xia, X.; Wolynes, P. G. *Proc. Natl. Acad. Sci. U.S.A.* **2000**, *97*, 2990–2994.
(19) Dudowicz, J.; Freed, K. F.; Douglas, J. F. *Adv. Chem. Phys.* **2008**, *137*, 125–222.
(20) Buchenau, U.; Zorn, R. *Europhys. Lett.* **1992**, *18*, 523–528.
(21) Scopigno, T.; Ruocco, G.; Sette, F.; Monaco, G. *Science* **2003**, *302*, 849–852.
(22) Sokolov, A. P.; Rössler, E.; Kisliuk, A.; Quitmann, D. *Phys. Rev. Lett.* **1993**, *71*, 2062–2065.
(23) Buchenau, U.; Wischnewski, A. *Phys. Rev. B* **2004**, *70*, 092201.
(24) Novikov, V. N.; Sokolov, A. P. *Nature* **2004**, *431*, 961–963.
(25) Novikov, V. N.; Ding, Y.; Sokolov, A. P. *Phys. Rev. E* **2005**, *71*, 061501.
(26) Yannopoulos, S. N.; Johari, G. P. *Nature* **2006**, *442*, E7–E8.
(27) Dyre, J. C. *Rev. Mod. Phys.* **2006**, *78*, 953–972.
(28) Larini, L.; Ottochian, A.; De Michele, C.; Leporini, D. *Nat. Phys.* **2008**, *4*, 42–45.
(29) Ottochian, A.; Leporini, D. *Philos. Mag.* **2011**, *91*, 1786–1795.
(30) Ottochian, A.; De Michele, C.; Leporini, D. *J. Chem. Phys.* **2009**, *131*, 224517.
(31) De Michele, C.; Del Gado, E.; Leporini, D. *Soft Matter* **2011**, *7*, 4025–4031.
(32) Ottochian, A.; Leporini, D. *J. Non-Cryst. Solids* **2011**, *357*, 298–301.
(33) Prevosto, D.; Capaccioli, S.; Lucchesi, M.; Leporini, D.; Rolla, P. *J. Phys.: Condens. Matter* **2004**, *16*, 6597–6608.
(34) Andreozzi, L.; Giordano, M.; Leporini, D. *J. Non-Cryst. Solids* **1998**, *235*−*237*, 219–224.
(35) Andreozzi, L.; Faetti, M.; Giordano, M.; Leporini, D. *J. Phys.: Condens. Matter* **1999**, *11*, A131–A137.
(36) Leporini, D.; Schädler, V.; Wiesner, U.; Spiess, H.; Jeschke, G. *J. Chem. Phys.* **2003**, *119*, 11829–11846.
(37) Baschnagel, J.; Varnik, F. *J. Phys.: Condens. Matter* **2005**, *17*, R851–R953.
(38) Andersen, H. C. *J. Chem. Phys.* **1980**, *72*, 2384–2393.
(39) Nosé, S. *J. Chem. Phys.* **1984**, *81*, 511–519.
(40) Tuckerman, M. E.; Berne, B. J.; Martyna, G. J. *J. Chem. Phys.* **1992**, *97*, 1990–2001.
(41) Trotter, H. F. *Proc. Am. Math. Soc.* **1959**, *10*, 545–551.
(42) Tuckerman, M. E.; Berne, B. J.; Martyna, G. J. *J. Chem. Phys.* **1991**, *94*, 6811–6815.
(43) Hansen, J. P.; McDonald, I. R. *Theory of Simple Liquids*, 3rd ed.; Academic Press: New York, 2006.
(44) Boon, J. P.; Yip, S. *Molecular Hydrodynamics*; Dover Publications: New York, 1980.
(45) Gedde, U. W. *Polymer Physics*; Chapman and Hall: London, 1995.
(46) Barbieri, A.; Campani, E.; Capaccioli, S.; Leporini, D. *J. Chem. Phys.* **2004**, *120*, 437–453.
(47) De Michele, C.; Leporini, D. *Phys. Rev. E* **2001**, *63*, 036701.
(48) Doi, M.; Edwards, S. F. *The Theory of Polymer Dynamics*; Clarendon Press: Oxford, 1988.
(49) Note that the alternative definition via the familiar relation $F_s(q,\tau_q) = 1/e$ cannot be used due to the strong q-dependence of the plateau region of the ISF function at intermediate times (see Figure 2). When $q \sim 2\pi/\sigma$, $\tau_q^{(0.1)} \sim \tau_\alpha^{(0.1)} \propto \tau_\alpha$ according to Figure 3, top panel.
(50) Durand, M.; Meyer, H.; Benzerara, O.; Baschnagel, J.; Vitrac, O. *J. Chem. Phys.* **2010**, *132*, 194902.